High precision astrometry and photometry on binary stars acquired with PUEO

Jean-Pierre Véran[1], Jean-Luc Beuzit[2], Diana Chaytor[2,3]
[1] Dominion Astrophysical Observatory, Victoria, BC, Canada
[2] Canada-France-Hawaii Telescope, Kamuela, HI, U.S.A.
[3] University of Victoria, Victoria, BC, Canada

Abstract

Observations of multiple star systems have tremendously benefitted from the high spatial resolution achieved by adaptive optics. Still, even for binary stars, extracting the precise position (astrometry) and magnitude (photometry) difference between the two companions remains a difficult problem owing to the spatial extension and the time fluctuations of the AO PSF. In this paper, we present the methodology we are using for data acquired with PUEO, the Canada-France-Hawaii Telescope AO system. In a first stage, the AO PSF associated with each AO corrected image is estimated using the control loop data. In a second stage, this estimated PSF is used to deconvolve the AO image and obtain the position and magnitude of the two companions. We illustrate our method on several examples, using both real and simulated data, and assess its performance and robustness, demonstrating milliarc-second and percent accuracy, respectively for astrometry and photometry.

1 Introduction

When observing double or multiple stellar systems, adaptive optics provides the great advantage of being able to image closer and fainter companions than with traditional seeing-limited observations. Although actually detecting new companions is already of great interest, the ability to determine their relative position (astrometry) and magnitude (photometry) is of even greater interest, since it allows to derive the orbital elements of the systems and therefore the masses of the stars. This however is not easy to do. Indeed, even if the adaptive optics point spread function (PSF) very often has a diffraction-limited central core, providing the very high spatial resolution, it also features a significant fraction of the total flux scattered far out in the wings, giving a halo surrounding the central peak. In the case of a binary system, the image of the companion is usually super-imposed with the halo of the primary star. Beside a reduced contrast, this results in a strong bias, when using traditional centroiding and aperture photometry methods. More powerful deconvolution methods, such as PSF fitting methods, must be used in order to extract accurate astrometry and photometry. These methods however usually rely on the accurate knowledge of the PSF. In AO imaging however, the estimation of the PSF is a real problem as it is known to vary very quickly, with seeing and observing conditions. Another approach is to use even more sophisticated techniques called blind deconvolution, that does not need the knowledge of the PSF. But these methods are known to be less robust and more difficult to implement.

One of the unique features of PUEO, the Canada-France-Hawaii Telescope (CFHT) AO system, is that for most observations, the PSF can be accurately retrieved from the wave-front sensor data recorded during each acquisition. For this reason, PUEO observations are best processed in two steps: first the PSF is reconstructed, and second the astrometry and photometry are derived using robust schemes based on the knowledge of the PSF. The goal of this paper is to investigated the robustness and accuracy of this procedure, considering that the estimated PSF is never perfectly accurate.

The rest of the paper is organized as follows. In section 2, we review the steps required to process the PUEO data (cosmetic reduction, PSF retrieval and deconvolution). In section 3, we assess the performance of this technique, both on real and simulated data.

2 PUEO data processing steps

2.1 Cosmetic reductions

Cosmetic data reductions are not really specific to adaptive optics and are therefore just briefly mentionned here for the sake of completeness. They usually involve, for each frame, sky background subtraction, flat-fielding, correction of bad pixels, as well as correction for systematic detector effects such as the suppression of the remaining 60 Hz correlated noise. Then several frames can be combined to increase the signal-to-noise ratio.

2.2 PSF retrieval

At CFHT, tools have been developed to provide an accurate estimate of the AO corrected long-exposure point spread function *in the direction of the guide source, when the guide source is of magnitude 13 or brighter* [5] [3]. The magnitude and direction limitations do not really matter as binary systems of interest are usually bright and can be used as their own reference. The estimation / reconstruction process takes place partly on-line, partly off-line.

On-line computations For each exposure taken with PUEO, the following quantities are computed in real time, based on the wave-front sensor measurements and on the commands sent to the deformable mirror:

- The uncorrected free atmospheric seeing.
- The AO corrected long exposure "atmospheric PSF" that is the PSF that would have been obtained with a perfect telescope / optical train and a turbulence following the Kolmogorov model at high spatial frequencies

Off-line computations The actual PSF differs from the atmospheric PSF due to the following effects:

- Uncorrected non-common path aberrations
- High spatial frequency aberrations not following the Kolmogorov model such as mirror seeing or polishing defects.

Usually, these effects can be considered as quasi-static and thus can be calibrated using the image of a point source, taken sometimes during the night, e.g. a photometric standard [6]. CFHT provides a software called DPH2PSF that allows to compute the actual PSF from the atmospheric PSF. Because this software requires at least one *reduced* image of a point source, this computation is performed off-line by the observers. The DPH2PSF package, along with more detailled information on the PSF reconstruction with PUEO, are available from the web address: `http://www.cfht.hawaii.edu/manuals/aob/psf_dph.html`.

The error on the estimated PSF is of the order of a few percents on the low and medium frequencies of the modulation transfer function (MTF) increasing up to ten percents at the highest spatial frequencies [5]. However, how these errors propagate onto the astrometry and photometry measurements has not been studied yet. This is the goal of this paper.

2.3 Deconvolution: astrometric and photometric measurements

When the PSF is known, numerous deconvolution methods exist to remove the blur in the image. Widely used general methods include linear methods such as inverse or Wiener filtering, or non-linear methods such as Richardson-Lucy and Maximum Entropy, the latter being non-linear, slower but more robust than the former. It is important to point out here that the goal of the deconvolution process is not to increase the resolution of the image, as it is already diffraction-limited, but rather to reconcentrate the light from the wings into the central core, to avoid overlapping between the sources.

	PSF1	PSF2	PSF3
Visible magnitude	10.4	12.1	12.7
Estimated r_0 (cm)	18.7	15.4	19.8
Imagery wavelength (μm)	2.12	1.65	1.65
Real Strehl (%)	62.2	32.1	45.2
Estimated Strehl (%)	63.6	33.3	41.8

Table 1: Numerical values for the three chosen PSFs.

Still, stellar images are made of images of point sources but this additional strong information is not taken into account in the techniques mentionned above. Then, it is not surprising that methods that specifically assume images containing nothing but point sources perform significantly better. Such methods include DAOPHOT [2] and AOPHOT [4] and have already been used to process AO star cluster images. We chose to use AOPHOT because of the additional advantage to be specifically suited to the usual oversampling nature of AO images.

3 Performance

The performance of AOPHOT has already been assessed on star clusters [4] and it was shown that if the correct PSF is fed to the program, the error is very small on bright stars. Here, we are interested on the performance of the combined operation (PSF retrieval + AOPHOT) on binary stars. This performance is first assessed on simulated data, using real PSF and then compared to results obtained using real data.

3.1 Simulated data

We chose three different PSFs, for which we have the real (measured) PSF as well as the reconstructed PSF. PSF1 is a bright star and an example of excellent correction. PSF2 is an example of a typical correction in bad seeing. PSF3 is an example of a typical correction in good seeing. Numerical values for these PSFs are given in table 1. Graphic comparisons between the real and reconstructed PSF are given in reference [5] for PSF1 and PSF3 and in figure 1 for PSF2.

We have simulated binary systems with separation between $0.05''$ and $1.2''$ and magnitude difference 0, 1, 2, 3, 4 and 5. For each PSF and each magnitude difference, we use the real PSF to generate a binary system with a random separation and a random angle. We then provide the estimated PSF to the AOPHOT software and obtain an estimated separation and magnitude difference. These are compared to the real separation and magnitude difference in figures 2 and 3.

As expected, the performance degrades as the companion gets fainter and closer to the primary star. However, we show that for bright companions (not fainter than 10% of the primary star) at separation greater than $0.4''$, a photometric accuracy of a few percents in magnitude and an astrometric accuracy of a few milliarc-seconds can be achieved. Peculiar oscillations appear when the companion is very close to the primary star, increasing in amplitude as the companion gets fainter. These are due to the diffraction rings of the primary star.

3.2 Real data

As part of a program to improve the determination of the mass/luminosity relation for low mass stars ($< 0.3\mathrm{M}_\odot$) a team of astronomers from Observatoire de Grenoble, Observatoire de Genève and CFHT is systematically observing a sample of nearby M dwarf binary systems in order to very accurately derive their orbital elements, and therefore their masses [1]. The goal is to determine the masses with errors in the range of 2 to 5%, as compared to the current 10 to 30%. The orbital elements are obtained by combining highly accurate radial velocities (10-70 m/s) measured

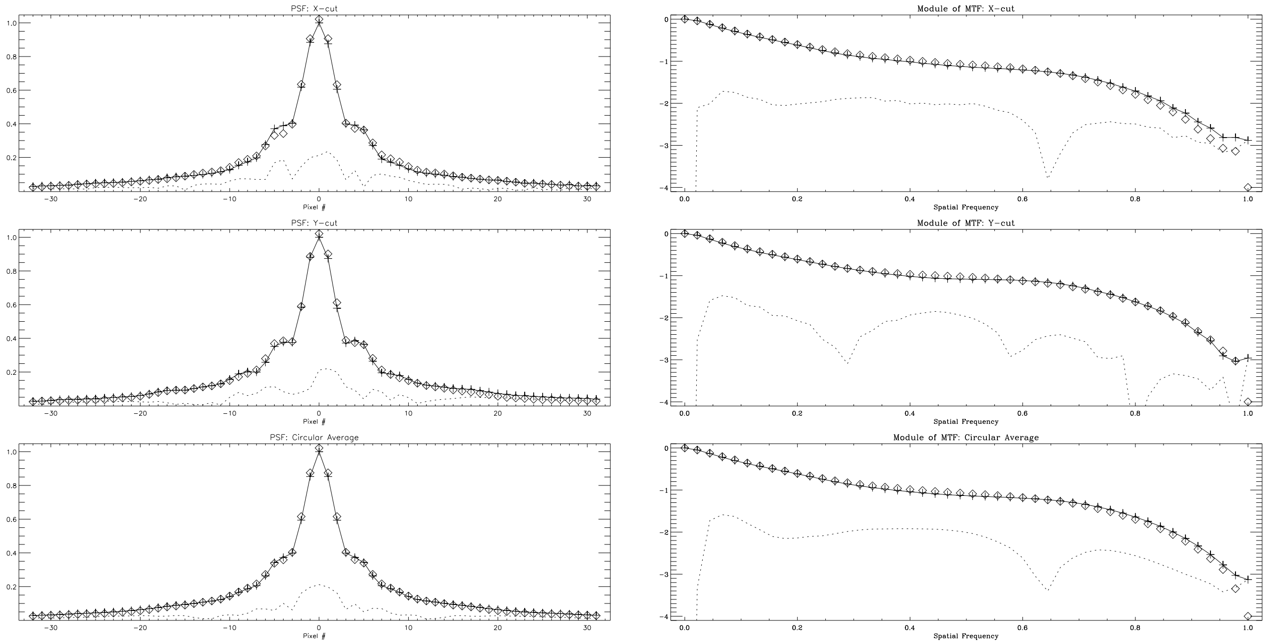

Figure 1: Comparison between the estimated PSF and the real PSF. Left: image, vertical scale is square root. Right: modulation transfer function, vertical scale is logarithmic. Top graph: X-cut, middle graph: Y-cut, bottom graph: circular average. The vertical scale is square root. The real PSF is shown in solid line and plus signs. The estimated PSF is shown in diamond signs. The dot line is the absolute difference of the two curves, plotted with the same vertical scale.

with the ELODIE spectrograph at Observatoire de Haute-Provence (France) and diffraction-limited images obtained in the near-infrared with the PUEO adaptive optics system at CFHT.

The data used for the present study were obtained in July 1998 with PUEO and its dedicated infrared camera KIR. To improve the S/N ratio and to average the residual uncorrected atmospheric turbulence, series of $\sim$ 4 minutes total integration times per filter were accumulated in a four position mosaic pattern. For each filter, the raw images were median combined to obtain sky frames which were then subtracted from the raw data. Subsequent reduction steps included flat-fielding, correction of the bad pixels and shift-and-add combination of the corrected frames to produce the final images. Examples of the reduced images are presented in figure 4.

The estimated PSF corresponding to each of the final images was reconstructed from the atmospheric PSF using the DPH2PSF package. Finally, for each set of infrared images and estimated PSF, the AOPHOT software was used to extract the astrometric (separation and position angle) and photometric (difference in magnitude) parameters of the binary systems. The results are summarized in table 2 for all objects observed on July 22, as a function of their magnitude in the visible. The seeing was very stable during the night, with a median value of 0.6". The errors on the separation, position angle and difference in magnitude are compared with the simulated data in figures 2 and 3 and found to be in good agreement.

4 Conclusion

In this paper, we have assessed the accuracy with which the astrometry and photometry of binary stars observed with PUEO can be determined, as a function of the separation and magnitude difference of the companion. The processing technique we have used is a two-step method. First, the PSF associated with each image is reconstructed using CFHT on-line and off-line tools. Second, this PSF is used in conjonction with the AOPHOT program to extract the astrometry and the photometry. Using simulated data with real PSFs, we have found that when the companion

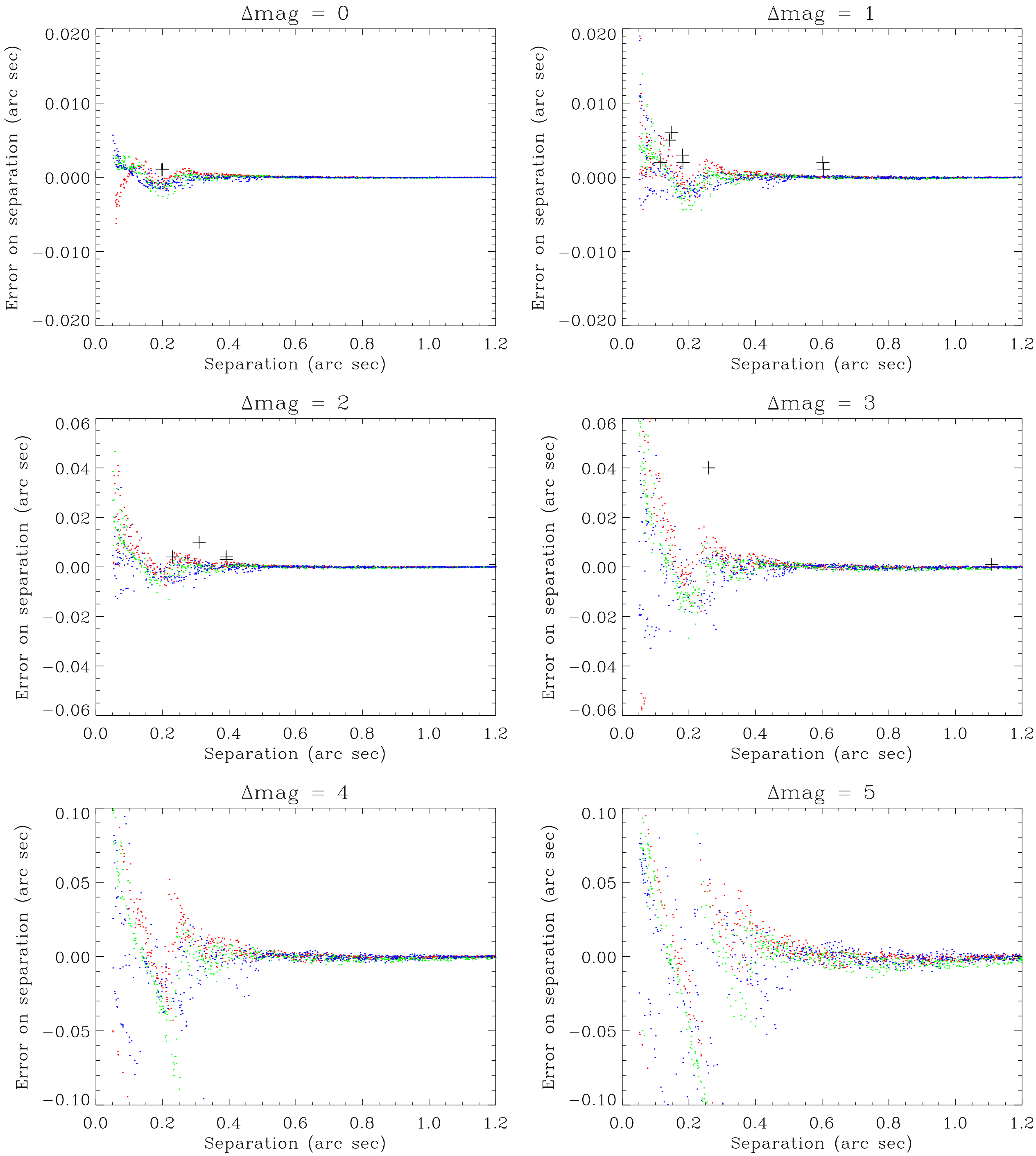

Figure 2: Error on the separation as a function of the separation for different magnitude differences. Blue: PSF1; green: PSF2; red: PSF3. The + signs are the experimental results from section 3.2.

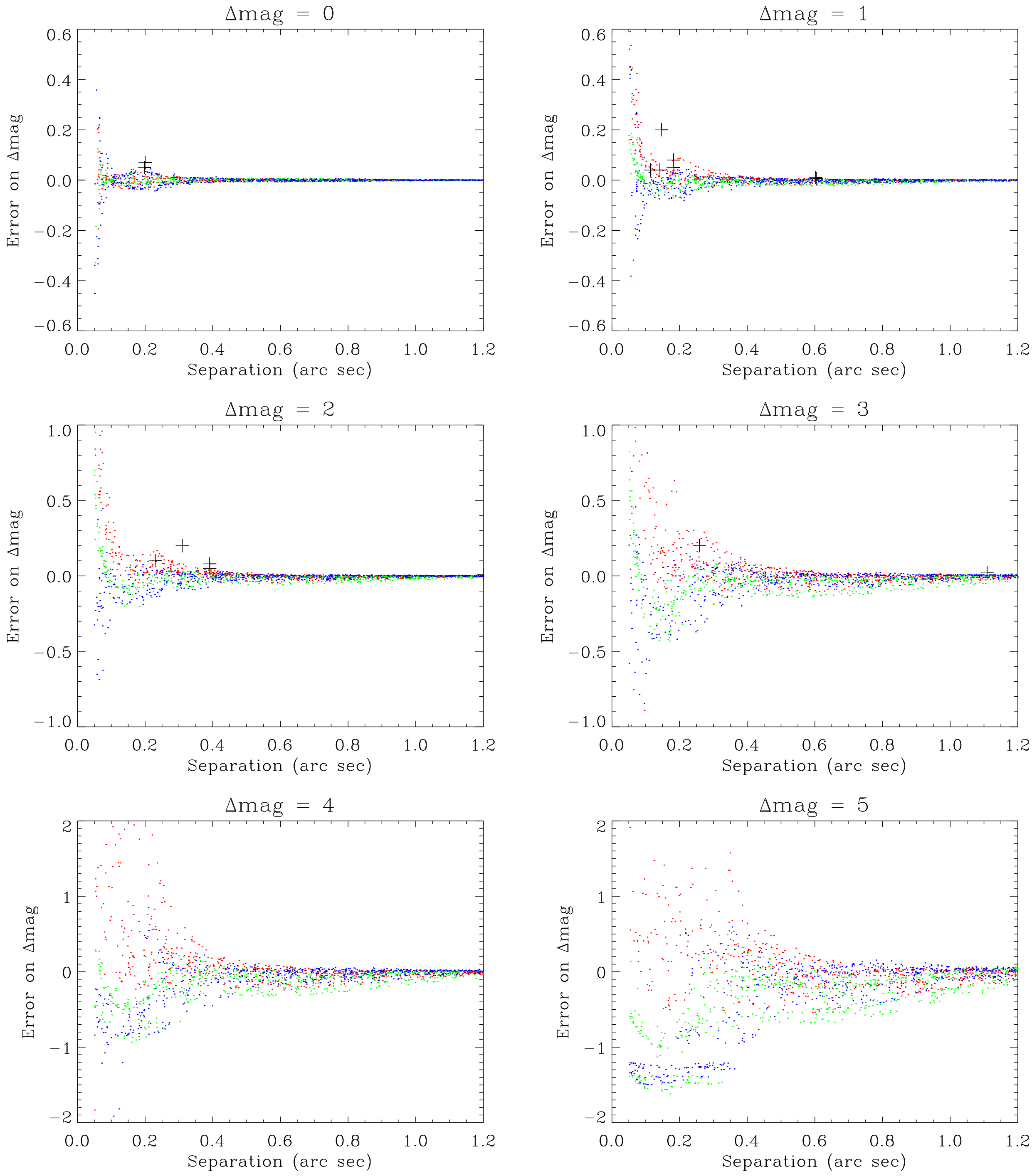

Figure 3: Error on the magnitude as a function of the separation for different magnitude differences. Blue: PSF1; green: PSF2; red: PSF3. The + signs are the experimental results from section 3.2.

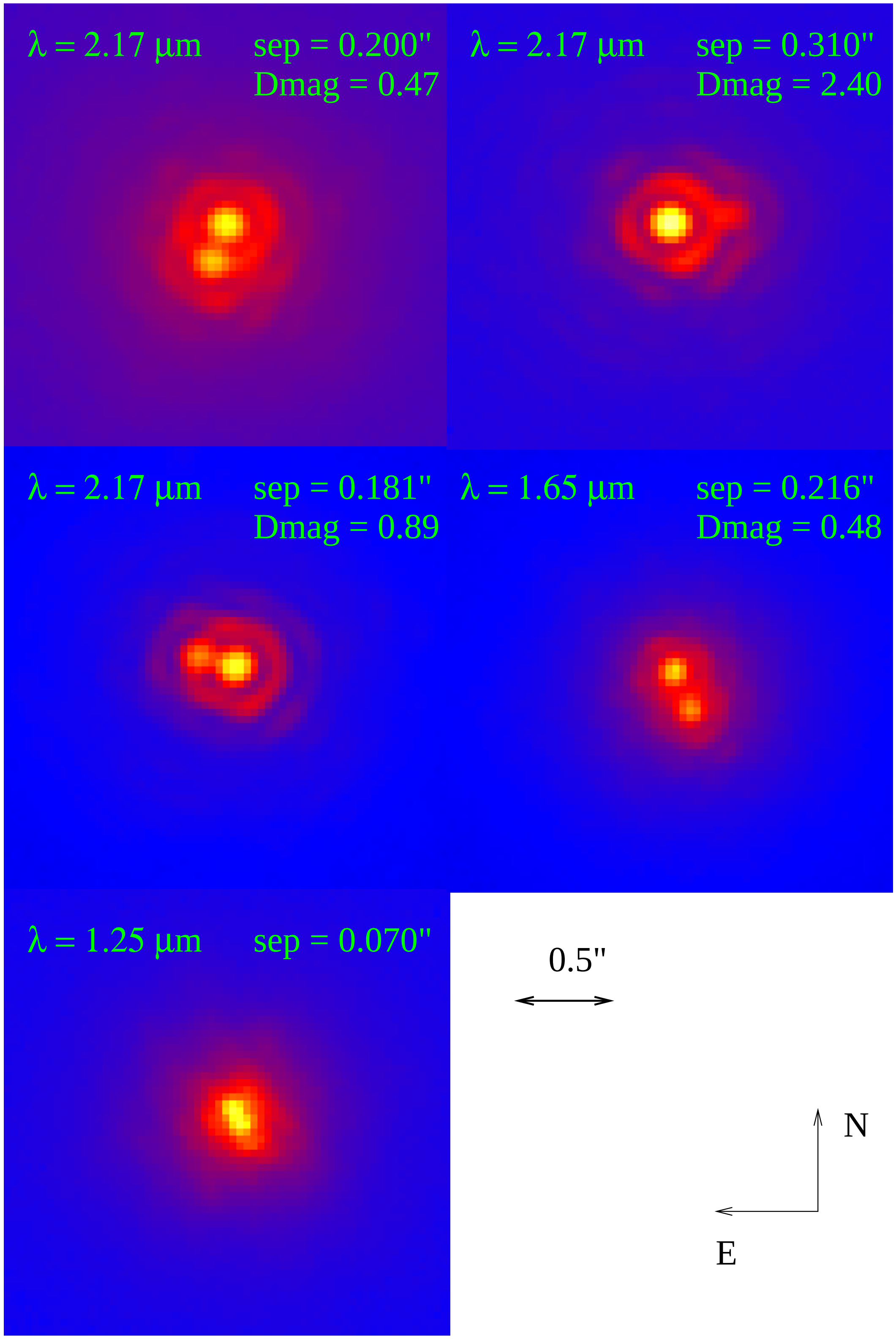

Figure 4: Examples of binary systems observed in July 1998 with PUEO and KIR.

m_R	Filter	ρ ($''$)	ρ err	PA (°)	PA err	Δ Mag	Mag err
5.50	Br γ	1.109	0.001	104.5	0.1	2.98	0.02
5.90	Br γ	0.181	0.003	73.3	0.3	0.89	0.05
	Fe II	0.182	0.002	72.8	0.7	1.01	0.08
6.75	Br γ	10.1100	0.0004	248.86	0.04	3.71	0.02
	Fe II	10.078	0.006	248.88	0.05	4.3	0.1
7.10	Br γ	0.31	0.01	276.3	0.3	2.4	0.2
	Fe II	0.230	0.004	275.0	0.9	2.4	0.1
7.50	Br γ	0.391	0.004	101.59	0.07	2.37	0.05
	Fe II	0.391	0.003	101.8	0.6	2.36	0.08
7.90	Fe II	1.226	0.001	105.9	0.1	2.34	0.01
8.00	Br γ	0.142	0.005	221.0	2.0	1.18	0.04
	Fe II	0.147	0.006	223.0	2.0	1.3	0.2
9.70	Fe II	0.216	0.002	201.9	0.3	0.48	0.06
10.3	Fe II	0.259	0.004	352.4	0.5	2.8	0.2
10.9	Fe II	0.114	0.002	305.2	0.9	0.72	0.04
	J	0.105	0.002	306.0	2.0	1.1	0.3
11.9	J	0.070	0.002	202.0	1.5	–	–
12.7	Br γ	0.200	0.001	155.9	0.9	0.47	0.07
	Fe II	0.198	0.001	156.2	0.7	0.41	0.05
13.5	Br γ	0.604	0.001	275.6	0.1	1.091	0.006
	Fe II	0.602	0.002	275.49	0.08	1.22	0.01
	J	0.609	0.001	275.6	0.1	1.40	0.01

Table 2: Results of the parameter extraction for the data obtained with PUEO on 22 July 1998.

is not fainter than 10% of the primary star and is situated more than $0.4''$ away, a photometric accuracy of a few percents in magnitude and an astrometric accuracy of a few milli arc-seconds can be achieved. This performance degrades smoothly as the companion gets fainter, and following an oscillating pattern due to the Airy rings of the primary star as the companion gets closer. These results have been confirmed on real observations of binary systems. The method will allow to determine the orbital elements of these systems, and therefore the masses of each of their components, with an accuracy of a few percents on a time scale of a few years.

References

[1] J.-L. Beuzit, X. Delfosse, T. Forveille, S. Udry, M. Mayor, C. Perrier, J.-M. Mariotti, and D. Segransan. Results obtained with both adonis and pueo on a study of low mass stars and a search for brown dwarfs. In *Astronomy with Adaptive Optics*, ESO Conference and Workshop Proc., 1998. (this volume).

[2] P.B. Stetson. DAOPHOT - a computer program for crowded-field stellar photometry. *Publ. Astr. Soc. Pac.*, 99:191–222, 1987.

[3] J. Thomas, G. Barrick, and J.-L. Beuzit. Experiences operating cfht's adaptive optics system. In D. Bonaccini and R. K. Tyson, editors, *Adaptive Optical System Technologies*, volume 3353 of *Proc. SPIE*, pages 94–100, 1998.

[4] J.-P. Véran and F. Rigaut. A deconvolution method for accurate astrometry and photometry on adaptive optics images of stellar fields. In D. Bonaccini and R. K. Tyson, editors, *Adaptive Optical System Technologies*, volume 3353 of *Proc. SPIE*, pages 426–437, 1998.

[5] J.-P. Véran, F. Rigaut, H. Maître, and D. Rouan. Estimation of the adaptive optics long exposure point spread function using control loop data. *J. Opt. Soc. Am. A*, 14(11), 1997.

[6] J.-P. Véran, F. Rigaut, H. Maître, and D. Rouan. Estimation of the adaptive optics long exposure point spread function using control loop data: recent developments. In *Adaptive Optics and Applications*, volume 3126 of *Proc. SPIE*, pages 81–92, 1997.